

# A Method for Folding Origami Rectilinear Polygon Extrusions

## **Abstract**

We present a method for generating crease patterns for folding any rectilinear polygon extrusion with a specified uniform minimum edge-to-edge distance, using a rectangular sheet of paper. We demonstrate that the resulting models are efficient and watertight. In addition, they achieve optimal efficiency, meaning they attain the smallest possible scale factor from the original sheet of paper to the folded rectilinear polygon extrusion. Finally, we provide a code implementation of the method. Our study not only facilitates crease pattern design for origami artists but also offers an innovative, art-driven pedagogical tool for inspiring interest in mathematics.

## 1 Introduction

Origami is the traditional Japanese art of paper folding. Originally practiced as a creative art form, origami is now widely studied for its mathematical properties. The geometry and topology inherent in origami make it particularly well-suited for mathematical investigation and practical applications; for example, one can produce precise angles in a sheet of paper using specific combinations of folds (Lang, 2010). Moreover, geometric analyses of origami crease patterns can help uncover methods for folding a model with prescribed dimensions using the smallest possible sheet of material, that is, in the most efficient way. Since designs made from one flat sheet of material, like paper or sheet metal, are often more materially efficient than those using multiple pieces linked by hinges or joints, origami has also inspired numerous engineering advancements, such as the expandable solar arrays developed by Zirbel et al. (2015).

All origami models can be folded with only two basic folds: mountain folds and valley folds, which are shown in Figures 1 (a) and (b), respectively, with the former shown in red and latter in blue. More complicated folds, such as reverse folds, pleats, or sinks, are combinations of mountain and valley folds. All crease patterns discussed in this paper only utilize these two basic folds.

Many properties of origami models, including their efficiency and even the foldability of their crease patterns, are constrained by the choice of materials, folding methods, and underlying geometric principles. For example, as we prove later in the paper, the crease patterns created using our method are the most efficient out of any hypothetical alternatives that create the same models. The existence of such constraints on an origami model suggests that origami designs can be systematically analyzed and quantified, potentially making them instrumental for math education and research.

The quantitative nature of origami highlights the valuable role that computational techniques can play in its design. Computational origami now presents opportunities for designing foldable, complex, and efficient structures using fundamental

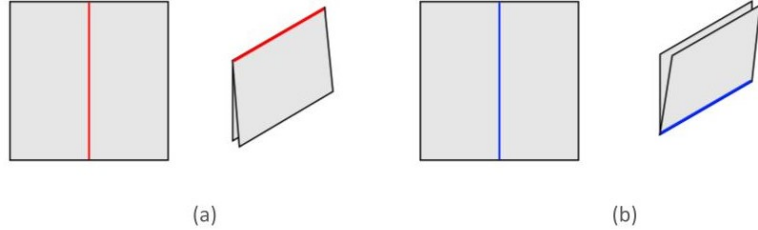


**Fig. 1 Example of mountain fold and valley fold.** The left panels of (a) and (b) show the crease pattern of a single mountain or valley fold, respectively, and the right panels show the folded models following these crease patterns. Mountain (valley) folds are commonly shown as red (blue) in crease patterns. These coloring schemes are followed in the rest of paper.

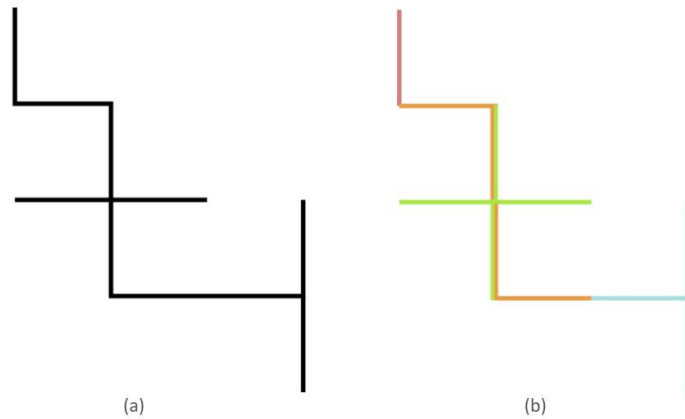


**Fig. 2 Example of breaking down a 2D graph into different gadgets.** (a) shows the 2D graph and (b) shows the layered gadgets. Each colored segment represents a different gadget with a different number of edge intersections. Line segments with multiple colors represent areas where different gadgets overlap.

building blocks. Researchers have explored this potential through algorithms that generate foldable crease patterns for orthogonal graphs. Demaine, Demaine, and Ku (2010) and Demaine, Ku, and Yoder (2018) develop origami algorithms to create orthogonal, triangular, and hexagonal graphs. These algorithms can take any 2D graph and generate a crease pattern for a corresponding 3D origami structure capable of forming mazes, paths, or even letters of the alphabet. The algorithms, which run in linear time relative to the number of nodes in the input graph, work by laying different “gadgets” onto the 2D graph, as shown in Figures 2 (a)-(b). These gadgets are folded 3D representations of all possible 2D edge intersections.

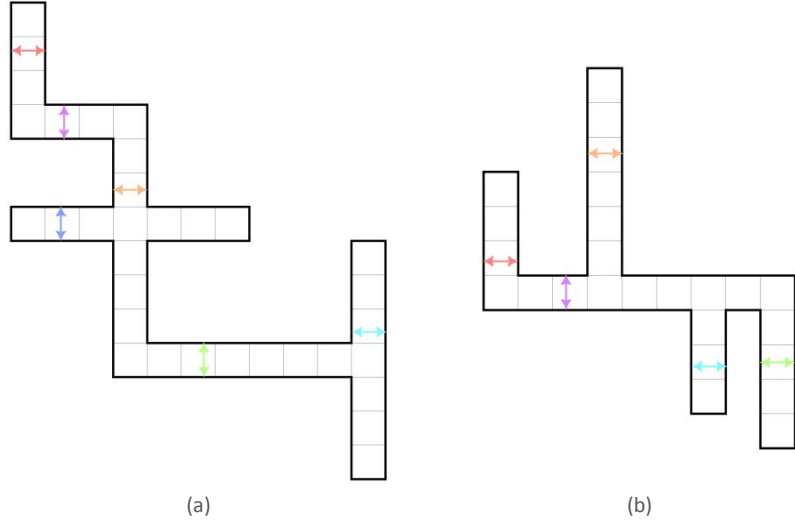


**Fig. 3 Sample cartoon top-down drawings of rectilinear polygon extrusions with a uniform minimum edge-to-edge distance.** In (a) and (b), the minimum edge-to-edge distances are illustrated by colored arrows. The constant length of all the arrows, i.e., the uniform minimum edge-to-edge distance, is defined as the *thickness* of a model. Individual *squares* in the rectilinear polygon extrusion are outlined in gray.

In general, this class of algorithms is evaluated by three key properties: *seamlessness*, *watertightness*, and *efficiency*.<sup>1</sup> *Seamlessness* refers to the condition where every visible face of the model consists of a single, uncreased layer of paper. *Watertightness* means that the model in its stable state (without glue, tape, or other materials) can hold water without leaking. *Efficiency* is quantified by the model’s scale factor, defined as the ratio between the dimensions of the original sheet of paper and those of the folded model. A smaller scale factor indicates a more efficient crease pattern.

In this paper, we present a method for generating crease patterns for folding any rectilinear polygon extrusion that has a uniform minimum edge-to-edge distance (Figures 3 a-b), using a single, uncut rectangular sheet of material. For brevity, we refer to the specific minimum edge-to-edge distance as the *thickness* of a model throughout the paper and formally define it in Section 2. Figure 4 presents a schematic of our method along with examples of folded origami models of letters. As shown in panels (a) and (b), the rectilinear polygon extrusions produced by

---

<sup>1</sup>We will formally define these properties in Section 2.

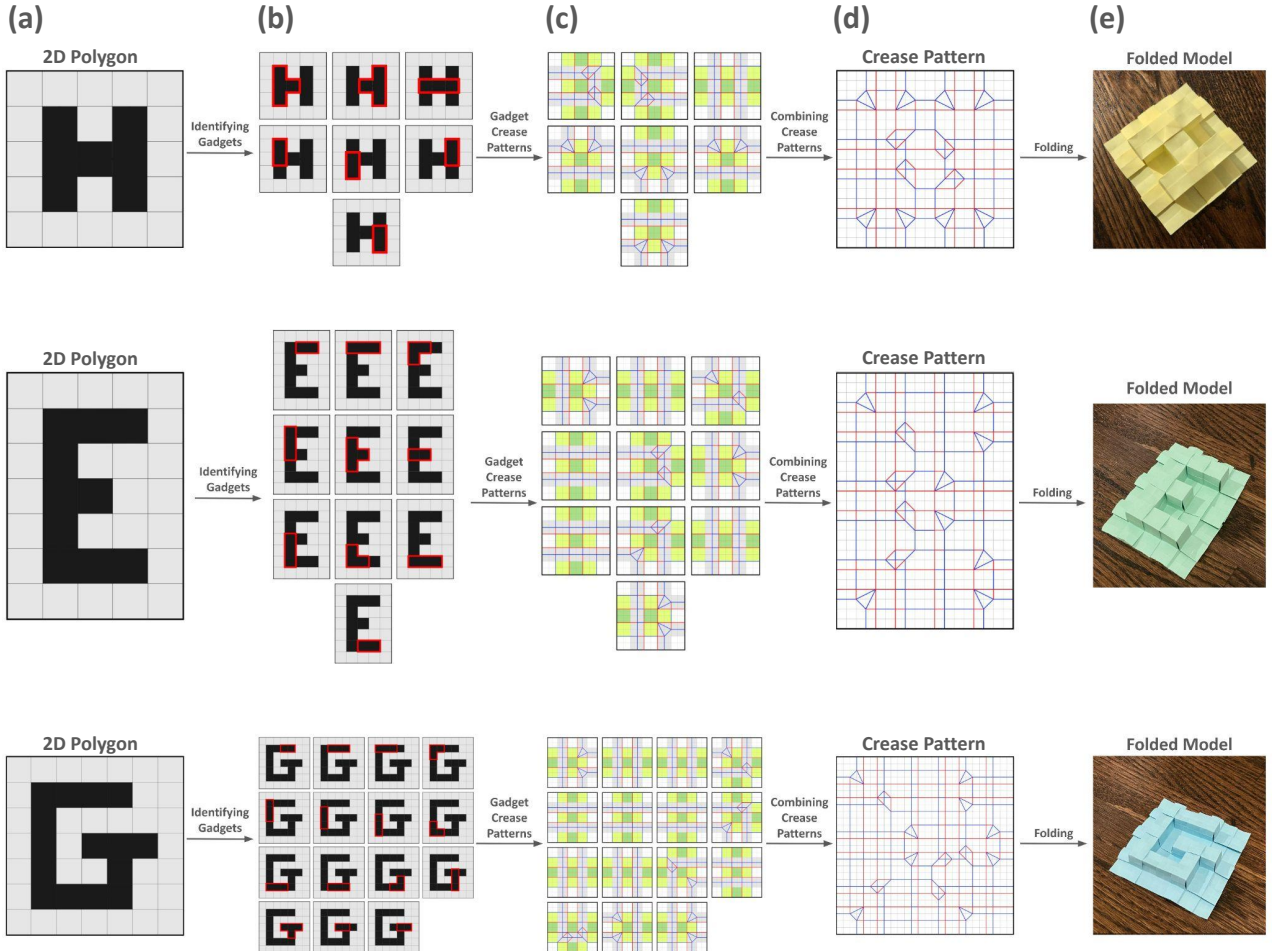


**Fig. 4 The schematic of our method.** The input 2D rectilinear polygon, division into gadgets, corresponding gadget crease patterns, output crease pattern, and folded model for each of the three rectilinear polygon extrusions (the letters “H,” “E,” and “G”) are shown. (a) shows the input 2D rectilinear polygon, where black regions represent extruded regions. (b) shows all the identified gadgets for each of the three rectilinear polygons, highlighted in red. (c) shows the crease patterns for the corresponding gadgets in (b). (d) shows the final crease pattern of each model. Finally, (e) shows the models folded according to the corresponding crease patterns.

our method are made up of individual *squares*. Specifically, our method first breaks each 2D rectilinear polygon down into different *gadgets*, or preset arrangements of squares (Figure 4 b). For each gadget, a crease pattern that forms a corresponding 3D extruded representation is then designed (Figure 4 c). By layering these smaller

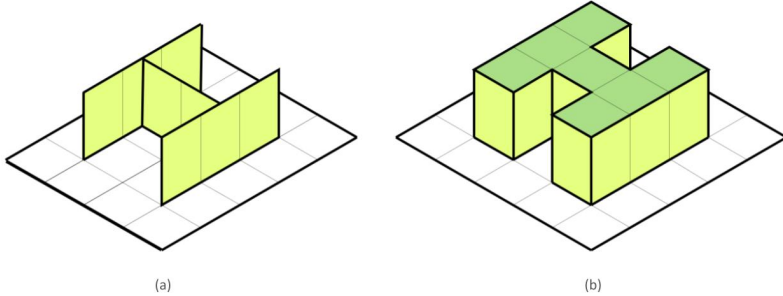


**Fig. 5 Comparison between a graph-based and rectilinear polygon origami model of “H.”** (a) shows the “H” created by the graph-based algorithm of Demaine, Demaine, and Ku (2010). (b) shows the rectilinear polygon “H” extrusion created by our method. The walls of the models are in yellow while the faces of the models are in green.

gadget crease patterns together, our method creates the overall crease pattern of the rectilinear polygon extrusion (Figure 4 d).

While all algorithms developed in prior studies are limited to 2D graph models, our method creates an extrusion of a rectilinear polygon resembling graph-like models with thickened edges. Figure 5 provides an example of a rectilinear polygon extrusion (the letter “H”) created by our method (Figure 5 b) in contrast to a similarly-shaped graph (Figure 5 a) generated by Demaine, Demaine, and Ku (2010).

The models produced under our method have optimal efficiency in that, for a given rectilinear polygon extrusion with a specified thickness (i.e., minimum edge-to-edge distance), they achieve the lowest scale factor possible (Demaine, Ku, and Yoder, 2018). The introduction of thickness into our gadgets adds an additional layer of complexity to the efficiency analysis because the scale factor now depends on both the thickness and height of extrusions.

These models are also watertight (Demaine and Tachi, 2017). Since they have no loose edges, they are able to hold water without leaking. Watertight models are generally deemed more practical to fold because they contain fewer regions with overlapping layers of paper. On the other hand, unlike graph-based models, models generated under our method are not seamless (Demaine, Ku, and Yoder, 2018).

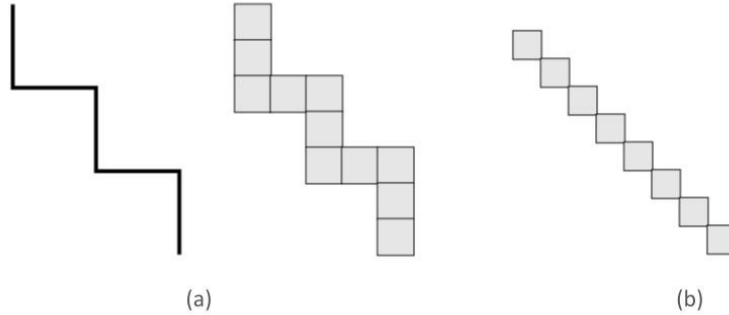


**Fig. 6 Different ways of creating a diagonal line using graphs and rectilinear polygons.** (a) shows a method of creating a diagonal line using a graph-based algorithm that is replicable using our rectilinear polygon-based method. (b) shows another method of creating a diagonal line that is unique to rectilinear polygon-based methods and cannot be created using graph-based algorithms.

This complication arises because our method generates rectilinear polygons with extruded faces. As we will prove in Section 4, it is impossible for any rectilinear polygon extrusion with a uniform minimum edge-to-edge distance to be completely seamless.

Additionally, our method can generate models unfoldable using graph-based algorithms. As shown in Figure 6 (a), different segments of models generated by graph-based algorithms must be continuous and connected orthogonally. However, our method can create continuous diagonal segments, as shown in Figure 6 (b). The individual squares shown in this figure can also be spaced further apart to create discrete, unconnected segments, which are also unfoldable using graph-based algorithms.

Lastly, to make our method more accessible to origami artists and math enthusiasts, we develop an automated implementation in Python, which is open-access through its GitHub link provided in Appendix B.

Our method provides an efficient technique for origami artists to generate custom patterns from 2D rectilinear polygons, whether those as standalone models, like the 3D letters in Appendix A, or as parts of larger origami works. In the latter case, because models generated using our method have the smallest scale factor

possible, they are the most materially efficient, making them ideal for integration with other origami components into more complex works.

Our method’s use of gadgets also makes it an effective pedagogical tool for origami design. Since it may be challenging to visualize repeating motifs in existing crease patterns, our use of gadgets as the building blocks to create larger models may be useful in the design process of repeating and/or symmetric origami bases, most notably present in traditional origami cranes and flowers.

Beyond implications for origami design, the models generated by our method can be used by mathematics educators to provide a visual and engaging exploration of geometric properties, from elementary concepts such as the volume and surface area of rectilinear polygon extrusions to more advanced topics such as the dimensional limits of certain models. In addition, proving additional properties of rectilinear polygon extrusions, beyond those presented in this paper, may serve as interesting mathematical exercises.

In Section 2, we formally define the basic terminologies in origami. Section 3 presents our method for generating foldable crease patterns corresponding to any rectilinear polygon extrusion with a uniform minimum edge-to-edge distance. Section 4 provides proofs for several properties of models generated by our method including their scale factor and seamlessness. Finally, Section 5 provides concluding remarks.

## 2 Definitions

Before developing our method, we formally define several standard origami-related terminologies that will be referenced throughout the rest of the paper.

**Definition 1** : A **mountain fold** is a fold that results in a crease protruding upward out of the paper and forming a “ridge,” relative to the original, flat sheet of paper. An example is shown in Figure 1 (a).

**Definition 2** : A **valley fold** is the opposite of a mountain fold, which results in a crease protruding downward and forming a “valley,” relative to the original, flat sheet of paper. An example is shown in Figure 1 (b).

**Definition 3** : A **seamless face** is a flat face in the folded model that is uncreased and consists of only one layer of paper. An example of a model with only seamless faces is shown in Figure 7 (a), and one that is similar but with only non-seamless faces is shown in Figure 7 (b).

**Definition 4** : A **seamless model** is a folded model in which all visible faces of the model are **seamless faces** (Demaine, Ku, and Yoder, 2018). Since many models contain at least one seamless face, a **seamless model** can also refer to a folded model where designated “major” faces of the model, e.g., the walls of folded rectilinear polygon extrusions, are seamless.

**Definition 5** : An **efficient model** is a model in which the scale factor from the dimensions of the unfolded sheet of paper to the dimensions of the folded model is reasonably small (Demaine, Ku, and Yoder, 2018).

**Definition 6** : An **optimally efficient model** is obtained when no other crease pattern associated with the same folded model can achieve a smaller scale factor from the unfolded paper to the folded model.

**Definition 7** : A **watertight model** is a model in which the boundaries of the folded model map to the boundaries of the original sheet of paper. In other words, the outer edge of the folded model is simply a collapsed version of the outer edge of the original sheet of paper. Figures 8 (a) and (b) illustrate a non-watertight model, and Figures 8 (c) and (d) illustrate a similar but watertight model.

**Definition 8** : In a folded rectilinear polygon extrusion, an **open end** is a region where a section of paper is part of the boundary of the unfolded paper but is *not* mapped to the boundary of the folded model. An example of an open end is shown

in Figure 9 (b), where the thick green line indicates the section of paper in question. No model with open ends is watertight.

**Definition 9** : In a folded rectilinear polygon extrusion, a **closed end** is a region where a section of paper is part of the boundary of the unfolded paper and is mapped to the boundary of the folded model. To be watertight, a folded rectilinear polygon extrusion must have closed ends only. An example of a closed end is shown in Figure 9 (c).

**Definition 10** : A folded rectilinear polygon extrusion is called **capped** if all ends are closed. All capped rectilinear polygon extrusions are watertight. Performing the specific set of folds that turns an open end into a closed one is called **capping** the end.

**Definition 11** : The **thickness** of a rectilinear polygon extrusion generated by our method refers to the polygon's uniform minimum edge-to-edge distance. Two examples of such rectilinear polygon extrusions are shown in Figure 3.

### 3 Method

The rectilinear polygon extrusions produced by our method are made up of individual *squares*. Our method generates crease patterns by using these squares as references for creating gadgets, like those shown in Figures 4 (b) and (c). Gadgets are small, folded extrusions that represent the set of all arrangements around a specific square in a 2D rectilinear polygon. As shown in (b), a gadget can be identified for every square in a 2D rectilinear polygon, with each gadget containing its own crease pattern. By layering the crease pattern of each gadget over the 2D rectilinear polygon, the crease pattern for a folded extrusion model resembling the 2D representation can be generated (Figure 4 d).

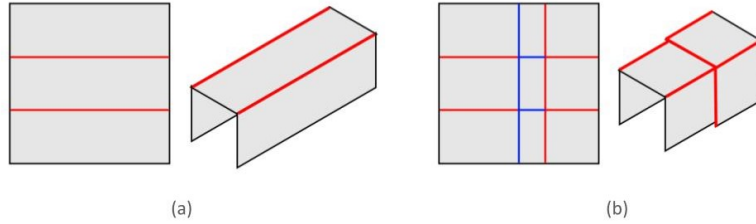


**Fig. 7 Examples of seamless and nonseamless models.** In panel (a), the faces are seamless because each face is uncreased (the only creases form the edges) and is covered by only one layer of paper. In panel (b), the faces are not seamless because they are covered by more than one layer of paper. Since every visible face in (a) is seamless, the model is also considered a seamless model.

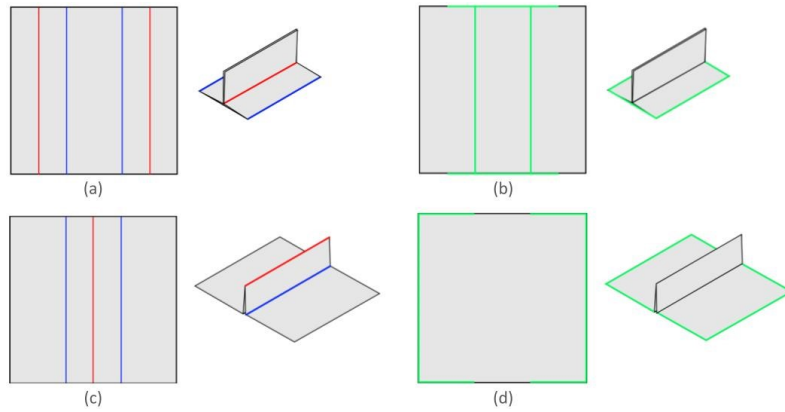


**Fig. 8 Examples of watertight and non-watertight models.** Panel (a) shows a non-watertight model's crease pattern. Panel (b) highlights in green the boundaries of the non-watertight, folded model, which do not fall along the edges of the original, unfolded paper. In contrast, panels (c) and (d) illustrate a watertight model whose boundaries fall along the edges of the original, unfolded paper.

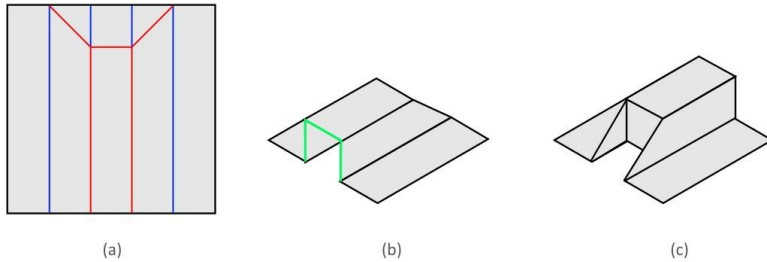


**Fig. 9 A model with both an open end and a closed end.** Panel (a) shows the crease pattern of a model with both an open end and a closed end. Panel (b) illustrates the open end, where the part highlighted in green is part of the boundary of the unfolded paper but not the boundary of the folded model. Panel (c) illustrates the closed end, where every part of the end is both part of the boundary of the unfolded paper and the boundary of the folded model.

### 3.1 Gadgets

Most properties of the folded rectilinear polygon extrusions, such as seamlessness and efficiency, depend on the properties of the gadgets themselves.<sup>2</sup> For instance, if a gadget is not seamless, a folded model using the gadget will not be seamless. The inverse statement, however, is not true. Even if all individual gadgets are seamless, a folded model may not always be seamless. This is because some properties of the folded rectilinear polygon extrusion also depend on the intersections between individual gadgets. If a folded rectilinear polygon extrusion is created with seamless gadgets but non-seamless gadget intersections, then it will not be seamless. However, our method is not affected by this slight nuance, as our gadget intersections are all seamless. This means that, for the folded rectilinear polygon extrusions generated by our method, their seamlessness only depends on the seamlessness of the gadgets.

The efficiency of a folded rectilinear polygon extrusion also depends on that of individual gadgets. The smallest possible scale factor from an unfolded sheet of paper to any folded rectilinear polygon extrusion is simply the scale factor of a single capped gadget, given that all the gadgets have the same scale factor. Otherwise, the smallest possible scale factor of any folded model would be that of the most efficient gadget.<sup>3</sup>

In rectilinear polygon extrusions with non-zero thickness, there are seven possible gadgets. Since our method’s polygons are rectilinear, in a given gadget, four possible squares can surround a central square. Thus, there should be  $2^4 = 16$  possible gadgets. However, after accounting for rotation, there are only 6 possible gadgets, plus one “special gadget,” where no other squares except the central

---

<sup>2</sup>Note that watertightness is not on the list of properties dependent on individual gadgets. This is because the watertightness of a model is *not* affected by the watertightness of the gadgets and only concerns the *boundary* of the folded model. In addition, any non-watertight gadget can be capped to form a watertight model.

<sup>3</sup>It is important, however, to note the distinction between the scale factor of an optimally efficient rectilinear polygon extrusion and the *smallest possible scale factor* of *any* folded rectilinear polygon extrusion. In fact, the vast majority of folded rectilinear polygon extrusions have an optimal scale factor greater than the smallest possible scale factor of *any* folded rectilinear polygon extrusions.

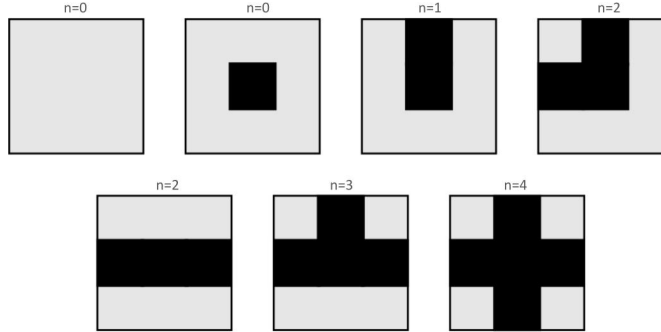


**Fig. 10** **The seven gadgets used in our method.** Filled-in, black squares indicate extruded regions. The number  $n$  above each gadget drawing indicates how many non-central squares are extruded in the gadget. The second gadget marked with  $n = 0$  is the “special gadget,” where no non-central squares are extruded but the center square is.

square are extruded. Figure 10 shows all seven gadgets, with the number  $n$  above each gadget drawing indicating the number of non-central squares that are extruded. However, in a single, continuous rectilinear polygon, as illustrated in Figure 4 (b), only the  $n = 1$  through  $n = 4$  gadgets are used.

Figure 11 presents the crease patterns of all seven gadgets used in our method. These crease patterns, with the exception of that for the special  $n = 0$  gadget, all have the same type of open ends as the one shown in Figures 9 (a) and (b). These open ends, as discussed later, can combine seamlessly (Figures 4 c and d). In our gadgets, a  $5 \times 5$  grid is folded to produce a  $3 \times 3$  gadget with varying numbers of extruded non-central squares. A common feature of all of our extruded gadgets is that the center square is always extruded (marked green in Figure 11), and that the four corners are always non-extruded (marked white in Figure 11); thus forming a  $3 \times 3$  gadget. The remaining squares are either collapsed layers or form the walls of the gadget; in either case, the scale factor of these gadgets remains the same.

### 3.2 Changing the Height of a Model

All the crease patterns shown in Figure 11 have a height-to-thickness ratio of 1:1; however, these crease patterns can be modified to have any desired height-to-thickness ratio. Two different techniques can be used to modify these crease

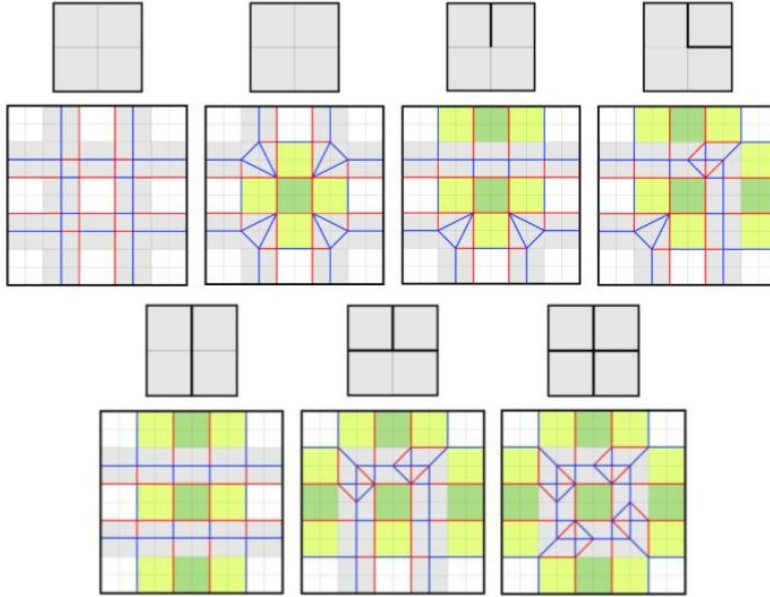


**Fig. 11 Crease patterns of the seven gadgets used in our method.** Green indicates an extruded face; yellow indicates a portion making up the side of an extruded square; white indicates a non-extruded portion; and gray indicates the collapsed regions of the paper. Red and blue lines indicate mountain and valley folds, respectively.

patterns: one involving box pleating and one without. Which of the two methods should be used depends on the specific height-to-thickness ratio desired.

The technique involving box pleating can be used for crease patterns with any height-to-thickness ratio, while the one without box pleating, which is also far simpler, can only be used for those with a height-to-thickness ratio less than or equal to 2:1. For these types of crease patterns, using the box-pleating technique is actually undesirable because it creates unnecessary complexity and thicker layers of paper, which can make the model harder to fold. Thus, the technique without box pleating is preferable and also results in a lower scale factor than the one with box pleating. We next discuss each of the two techniques employed to modify a crease pattern in more detail.

### 3.2.1 Height-to-thickness ratios of less than or equal to 2:1

As discussed earlier, to fold rectilinear polygon extrusions with height-to-thickness ratios of less than 1:1, e.g., 1:2 or 1:8, the modification technique without box pleating should be applied. Since it does not require sinks or box pleats, gadgets with different height-to-thickness ratios will have different scale factors. For example, a gadget with a height-to-thickness ratio of 1/2 would have a scale factor smaller than that of a gadget with a height-to-thickness ratio of 1:1, which is 5/3, as represented in Figure 11.<sup>4</sup>

Given that the smallest scale factor possible is 1, each one unit increase in a gadget's height-to-thickness ratio,  $h$ , increases its scale factor,  $s$ , by a value of  $\frac{5}{3} - 1 = \frac{2}{3}$ , as in Equation 1,

$$s = 1 + \frac{2h}{3}, h \in (0, 2] \quad (1)$$

To modify the crease pattern using this technique, the areas highlighted in yellow in Figure 11 can be stretched or shortened along the axis pointing away from the green squares. For example, the crease pattern of Figure 12 (a), which has a 1:1 height-to-thickness ratio as shown in Figure 12 (b), can be modified to form Figure 12 (c), which has a 2:1 height-to-thickness ratio.

Elongating or shortening the yellow squares affects the rest of the crease pattern minimally: only the other yellow areas or the gray collapsed areas of the paper are influenced. Certain collapsed areas, highlighted in orange in Figures 12 (b) and (c), remain as squares, even after scaling the yellow regions. This means that the sets of folds that collapse the paper in these orange regions remain the same, except that they will take up a different area. No matter how long or short the yellow regions are, these orange regions will always remain as squares.

---

<sup>4</sup>Specifically, the scale factor of a gadget with a height-to-thickness ratio of 1:1 is 5/3, because a 5 x 5 grid is folded to form a 3 x 3 gadget.

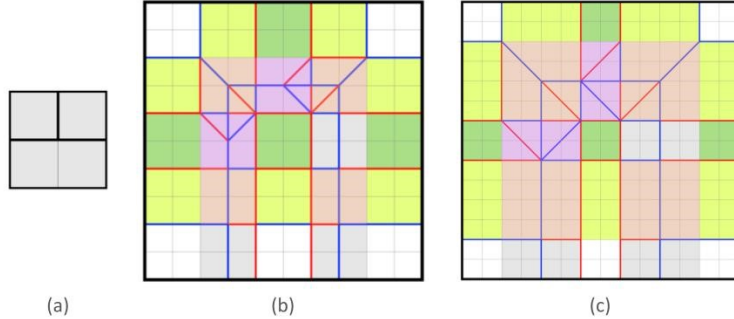


**Fig. 12 Comparison of the crease pattern between a two gadgets with identical structure but doubled height.** (a) shows a schematic representation of the gadget, (b) shows the crease pattern of the gadget with a 1:1 height-to-thickness ratio, and (c) shows the crease pattern of the same gadget but with a 2:1 height-to-thickness ratio. Green indicates an extruded face; yellow indicates a portion making up the side of an extruded square; and white indicates a non-extruded portion. Gray, orange, and purple regions indicate collapsed regions of the paper. Red and blue lines indicate mountain and valley folds, respectively.

However, other collapsed regions of the paper change in dimensions. This complicates the process by which a crease pattern is modified to achieve a new height-to-thickness ratio. Such areas are highlighted in purple in Figures 12 (b) and (c). For the gadget with a 1:1 height-to-thickness ratio, the region highlighted in purple is a square. However, for the gadget with a 2:1 height-to-thickness ratio, the same region is a two-by-one rectangle.

In order to collapse the paper properly, certain folds must appear in the purple region. Specifically, the purple region must contain both a mountain fold and a valley fold, with both extending from opposite corners on the right side of the purple region and intersecting at a 90-degree angle. In other words, the mountain fold, valley fold, and rightmost or uppermost boundary of the purple region should form a 45°-45°-90° triangle, with the mountain and valley folds as the legs and the boundary of the purple region as the hypotenuse. These folds must form the triangle strictly within the purple region and not extend outside (in the orange regions shown in Figures 12 b-c, for example). The single crease seen in the purple region of Figure 12 (b), which extends from the 90° vertex of the 45°-45°-90° triangle, is not necessary for proper collapsing of the hidden layers.

To meet the criteria outlined, the purple region must have at most a height-to-width ratio of 2:1. Since the height and width of the purple region are determined by the height of the walls of extruded squares (the yellow region) and thickness of the faces of extruded squares (the green region), this method of varying the thickness results in a collapsible model only if the height-to-thickness ratio also does not exceed 2:1.

### 3.2.2 Height-to-thickness ratios of greater than 2:1

To fold a rectilinear polygon extrusion with a height-to-thickness ratio of greater than 2:1, e.g., 4:1 or 6:1, box pleating must be employed to collapse the paper properly. This is because using the technique without box pleating to create height-to-thickness ratios greater than 2:1 has one critical issue. One valley fold, one mountain fold, and the rightmost or uppermost boundary of the purple-highlighted rectangle must form a  $45^\circ$ - $45^\circ$ - $90^\circ$  triangle strictly within the purple rectangle, as shown in Figures 12 (b) and (c). When a purple-highlighted rectangle's height-to-length ratio is greater than 2:1, the  $45^\circ$ - $45^\circ$ - $90^\circ$  triangle cannot fit within it. As a result, the crease pattern cannot properly collapse.

This issue with height-to-thickness ratios of greater than 2:1 can be solved by box pleating. As shown in Figures 13 (a) and (b), to effectively collapse the model, box pleating creates not one, but two  $45^\circ$ - $45^\circ$ - $90^\circ$  triangles within the purple rectangle. In other words, in the example shown in Figure 13 (b), box pleating splits the 4:1 purple rectangle into two 2:1 rectangles, which individually can be collapsed properly. However, the resulting crease patterns result in two times the thickness in the collapsed layers compared to those created by the non-box-pleating technique.

For any gadget with an  $h : 1$  height-to-thickness ratio, where  $h > 2$ , the purple-highlighted rectangle has dimensions of  $h$  by 1. Box pleating divides the  $h$  by 1 rectangle into  $p$  sets of  $j$  by 1 rectangles, where  $j \cdot p = h$  and  $j \in (0, 2]$ .  $p$  must also be an even number, or else the walls of squares (marked as yellow in Figure 13) will face inwards instead of outwards. The required number of box pleats can be

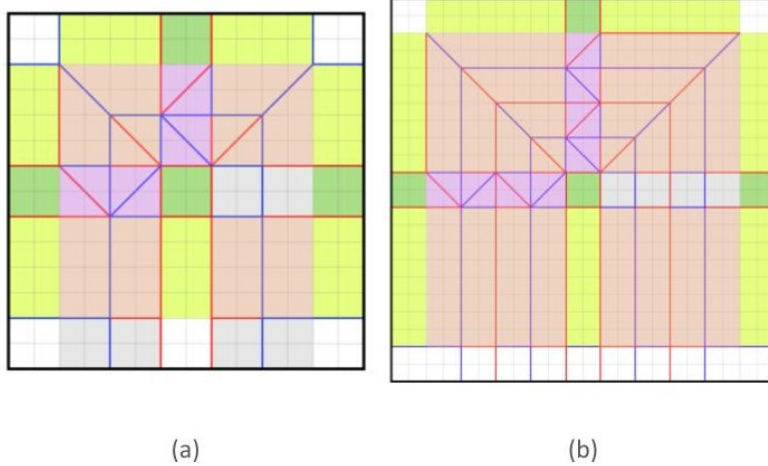


**Fig. 13 Comparison of the crease patterns for gadgets with varying height-to-thickness ratios.** (a) shows the crease pattern of a gadget with a 2:1 height-to-thickness ratio, and (b) shows the crease pattern of the same gadget but with a 4:1 height-to-thickness ratio. Green indicates an extruded face; yellow indicates a portion making up the side of an extruded square; and white indicates a non-extruded portion. Gray, orange, and purple regions indicate collapsed regions of the paper. Red and blue lines indicate mountain and valley folds, respectively.

modeled as a function of  $h$  as shown in Equation 2, where any gadget with an  $h : 1$  height-to-thickness ratio will require  $p$  box pleats to be foldable:

$$p = \lceil \frac{h}{4} \rceil \cdot 2 \quad (2)$$

Consequently, the number of paper layers in the model will increase by a factor of  $p$  as a result of the increased box pleating. The more one increases the height-to-thickness ratio of a gadget, the more paper layers will be present in the resulting extruded squares.

### 3.2.3 Scale factor of gadgets with varying height

Given that both modification techniques work for a height-to-thickness ratio of less than or equal to 2:1, we can derive the range within  $h \in (0, 2]$  in which a technique is most efficient (gives the smaller scale factor).

For the box pleating technique, the scale factor of any gadget with an  $h : 1$  height-to-thickness ratio, where  $h > 2$ , can be calculated using the number of box pleats required,  $p$ . The scale factor  $s$  is defined as follows:

$$s = 1 + \frac{2p}{3} \quad (3)$$

Substituting Equation 2 into Equation 3 yields

$$s = 1 + \frac{4}{3} \cdot \lceil \frac{h}{4} \rceil \quad (4)$$

For any  $h \in (0, 2]$ ,  $s = \frac{7}{3}$  when using the box pleating technique, according to Equation 4. Thus, the range under which the non-box-pleating technique is more efficient can be derived using the following inequality:

$$1 + \frac{2h}{3} \leq \frac{7}{3}, h \in (0, 2],$$

which holds true for all  $h \in (0, 2]$ . Thus, for all gadgets with a height-to-thickness ratio  $h \in (0, 2]$ , the non-box-pleating technique always produces models with the smaller scale factor and is thus always more efficient. Given that gadgets with a height-to-thickness ratio of  $h \in (2, \infty)$  can only be folded with box pleating, the smallest possible scale factor  $s$  for any gadget is defined as:

$$s = \begin{cases} 1 + \frac{2h}{3} & \text{if } h \in (0, 2] \\ 1 + \frac{4}{3} \cdot \lceil \frac{h}{4} \rceil & \text{if } h \in (2, \infty) \end{cases} \quad (5)$$

### 3.2.4 Changing the thickness of a model

Any desired increase in thickness can be achieved through a corresponding decrease in height. For example, a threefold increase in thickness corresponds to a threefold

decrease in height. Any modifications to the crease patterns using either one of the two techniques discussed earlier will alter the ratio between height and thickness, rather than the height or thickness individually.

### 3.3 Capping Open Ends of Gadgets

Any rectilinear polygon extrusion made up of layered gadgets will result in open ends around the border of the model because the gadgets themselves are uncapped. For each open end, the crease pattern shown in Figure 14 (a) can be applied to cap the end. From (b) to (c), only the end pointed upwards is capped; the ends that point laterally are still open (uncapped). If, for a given model, all its ends are capped, then the model as a whole will be watertight.

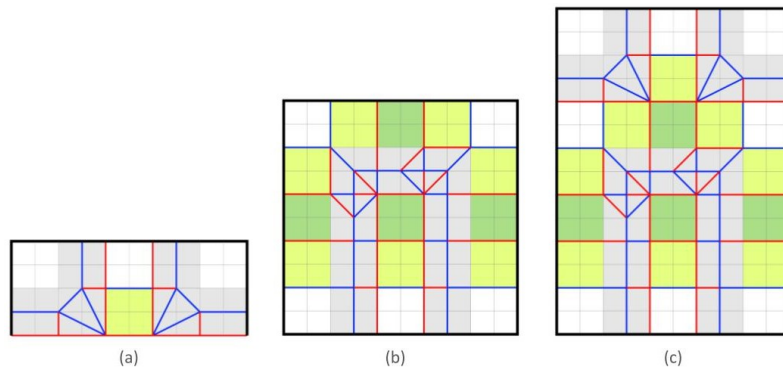


**Fig. 14** The process of capping an open end. (a) shows the crease pattern of the capping unit; (b) shows the crease pattern of the original gadget; and (c) shows the gadget in (b) with one end capped. Green indicates an extruded face; yellow indicates a portion making up the side of an extruded square; and white indicates a non-extruded portion. Gray regions indicate collapsed regions of the paper. Red and blue lines indicate mountain and valley folds, respectively.

The scale factor of a gadget is also affected by capping. Let  $n \in [0, 2]$  denote the number of capped lateral sides of a gadget, and  $m \in [0, 2]$  denote the number of capped vertical sides of the gadget. When adjusting Equation 5 for capping, the scale factor of a gadget will be different along the  $x$  and  $y$  directions:

$$s = (s_x, s_y)$$

$$s_x = \begin{cases} \frac{3+2h+(1+h)\cdot n}{3+n} & \text{if } h \in (0, 2] \\ \frac{3+\lceil \frac{h}{4} \rceil \cdot 4 + (1+h)\cdot n}{3+n} & \text{if } h \in (2, \infty) \end{cases}$$

$$s_y = \begin{cases} \frac{3+2h+(1+h)\cdot m}{3+m} & \text{if } h \in (0, 2] \\ \frac{3+\lceil \frac{h}{4} \rceil \cdot 4 + (1+h)\cdot m}{3+m} & \text{if } h \in (2, \infty) \end{cases}$$

which simplifies to

$$s = (s_x, s_y)$$

$$s_x = \begin{cases} 1 + h \cdot \frac{n+2}{n+3} & \text{if } h \in (0, 2] \\ 1 + \frac{\lceil \frac{h}{4} \rceil \cdot 4 + h \cdot n}{3+n} & \text{if } h \in (2, \infty) \end{cases}$$

$$s_y = \begin{cases} 1 + h \cdot \frac{m+2}{m+3} & \text{if } h \in (0, 2] \\ 1 + \frac{\lceil \frac{h}{4} \rceil \cdot 4 + h \cdot m}{3+m} & \text{if } h \in (2, \infty) \end{cases}$$
(6)

### 3.4 Connecting Gadgets

Figure 15 illustrates the method for combining gadgets: the two gadgets shown in Figures 15 (a) and (b) are connected to form the model shown in (c).

Every gadget has an identical crease pattern motif at its open ends. To connect two gadgets, two ends (one from each gadget) are overlapped by one unit, as shown in Figure 15 (c). Since the open end motifs are identical in every gadget crease pattern, all sets of gadgets can be connected using the method shown in Figure 15.

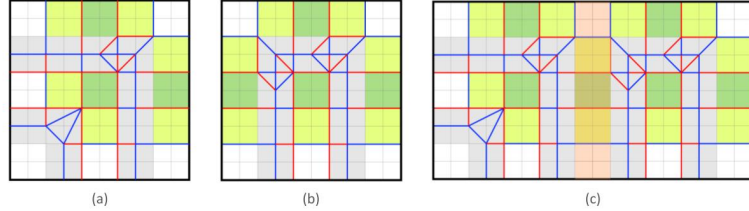


**Fig. 15 Example of combining two gadgets.** (a) and (b) illustrate the crease patterns of two different gadgets that are combined into (c). The region highlighted in orange is the overlapping region between the two gadgets. Green indicates an extruded face; yellow indicates a portion making up the side of an extruded square; and white indicates a non-extruded portion. Gray regions indicate collapsed regions of the paper. Red and blue lines indicate mountain and valley folds, respectively.

As no other parts of the gadgets, such as the collapsed regions, overlap, any set of connected gadgets can be folded and properly collapsed.

### 3.5 Scale factor of layered gadgets

As shown in Figure 4, each folded rectilinear polygon extrusion is made up of an  $a$  by  $b$  array of gadgets, which can also include empty gadgets. How the gadgets are connected influences the scale factor of the entire model.

The scale factor of a single gadget, taking into account height and capping, is shown in Equation 6. Taking into account the overlapping layers in gadget connections, the scale factor of an  $a$  by  $b$  array of gadgets is defined as follows:

$$s = (s_x, s_y)$$

$$s_x = \begin{cases} \frac{3+2h+(2h+2)\cdot(a-1)+(1+h)\cdot n}{3+2\cdot(a-1)+n} & \text{if } h \in (0, 2] \\ \frac{3+\lceil \frac{h}{4} \rceil \cdot 4 + (2h+2)\cdot(a-1)+(1+h)\cdot n}{3+2\cdot(a-1)+n} & \text{if } h \in (2, \infty) \end{cases}$$

$$s_y = \begin{cases} \frac{3+2h+(2h+2)\cdot(b-1)+(1+h)\cdot n}{3+2\cdot(b-1)+n} & \text{if } h \in (0, 2] \\ \frac{3+\lceil \frac{h}{4} \rceil \cdot 4 + (2h+2)\cdot(b-1)+(1+h)\cdot m}{3+2\cdot(b-1)+m} & \text{if } h \in (2, \infty) \end{cases}$$

which can be simplified to

$$s = (s_x, s_y)$$

$$s_x = \begin{cases} 1 + h \cdot \frac{2a+n}{2a+n+1} & \text{if } h \in (0, 2] \\ 1 + (h \cdot \frac{2a+n-2}{2a+n+1} + 2 \cdot \frac{\lceil \frac{h}{4} \rceil \cdot 2 - 1}{2a+n+1}) & \text{if } h \in (2, \infty) \end{cases}$$

$$s_y = \begin{cases} 1 + h \cdot \frac{2b+m}{2b+m+1} & \text{if } h \in (0, 2] \\ 1 + (h \cdot \frac{2b+m-2}{2b+m+1} + 2 \cdot \frac{\lceil \frac{h}{4} \rceil \cdot 2 - 1}{2b+m+1}) & \text{if } h \in (2, \infty) \end{cases}$$

This form shows how changes in gadget number, height, and capping increase the smallest possible scale factor of any model, 1.<sup>5</sup> The expression can be more cleanly simplified to:

$$s = (s_x, s_y)$$

$$s_x = \begin{cases} 1 + h - \frac{h}{2a+n+1} & \text{if } h \in (0, 2] \\ 1 + h - \frac{\lceil \frac{h}{4} \rceil \cdot 4 - 3h - 2}{2a+n+1} & \text{if } h \in (2, \infty) \end{cases}$$

$$s_y = \begin{cases} 1 + h - \frac{h}{2b+m+1} & \text{if } h \in (0, 2] \\ 1 + h - \frac{\lceil \frac{h}{4} \rceil \cdot 4 - 3h - 2}{2b+m+1} & \text{if } h \in (2, \infty) \end{cases}$$

(7)

---

<sup>5</sup>When a model contains no creases, its dimensions are the same as the original paper, hence a scale factor of 1.

This form is useful because the terms  $a$  and  $b$  are always in the denominators of fractions. Assuming  $h$  is a finite number, we can now place a limit on the largest scale factor possible for a folded rectilinear polygon extrusion, which occurs when  $a \rightarrow \infty$  and  $b \rightarrow \infty$ ; in other words, in an infinitely large rectilinear polygon extrusion. We can evaluate the largest possible  $s$ , which is that of an infinitely large rectilinear polygon extrusion, by applying limits to Equation 7 as the following,

$$\begin{aligned}\lim_{a \rightarrow \infty} s_x &= \lim_{b \rightarrow \infty} s_y \\ \lim_{a \rightarrow \infty} s_x &= \begin{cases} \lim_{a \rightarrow \infty} (1 + h - \frac{h}{2a+n+1}) & \text{if } h \in (0, 2] \\ \lim_{a \rightarrow \infty} (1 + h - \frac{\lceil \frac{h}{4} \rceil \cdot 4 - 3h - 2}{2a+n+1}) & \text{if } h \in (2, \infty) \end{cases} \\ &= 1 + h = \lim_{b \rightarrow \infty} s_y \\ s_\infty &= (\lim_{a \rightarrow \infty} s_x, \lim_{b \rightarrow \infty} s_y) \\ &= (1 + h, 1 + h)\end{aligned}$$

An infinitely large rectilinear polygon extrusion can be folded from an original sheet of paper with side lengths  $1 + h$  times larger than those of the folded rectilinear polygon extrusion. Thus, for any folded rectilinear polygon extrusion with finite side lengths, the scale factor  $s$  from the original sheet of paper to the folded rectilinear polygon extrusion is always less than  $1 + h$ .

## 4 Properties of Rectilinear Polygon Extrusions

In this section, we examine two key properties of rectilinear polygon extrusions: seamlessness and efficiency. One main difference between our method and those developed by Demaine, Demaine, and Ku (2010) and Demaine, Ku, and Yoder (2018), which generate graph-like models, is that our crease patterns are not folded

seamlessly. As shown in Figure 15, for example, the green squares are continuous in the folded model but contain collapsed layers in between them in the crease pattern; these collapsed layers create seams when folded properly. However, as we prove below, for rectilinear polygon extrusions with nonzero thickness, no seamless crease pattern exists, with the exception of rectilinear polygon extrusions without a single  $90^\circ$  vertex.

**Theorem 1** *No set of watertight, orthogonal gadgets with a thickness greater than zero and at least one  $90^\circ$  vertex can be seamless.*

*Proof* Consider the hypothetical crease pattern of a  $90^\circ$  vertex gadget without seams shown in Figure 16 (a) and its hypothetical folding shown in Figure 16 (b). Two white dots are marked as shown in the hypothetical folding, and their corresponding places in the hypothetical crease pattern are also marked. The thick blue line represents the intrinsic distance (distance along the creases in the folded model) between the two white dots, and the thick red line represents the shortest distance between the two points in the crease pattern.

To be foldable, the intrinsic distance must be less than or equal to the shortest distance in the crease pattern. This is because any intrinsic distance in the model cannot increase during the folding process (Demaine, Ku, and Yoder, 2018). The thick blue line and the thick red line form a triangle in Figure 16 (a), and by the triangle inequality, the intrinsic distance in the model is greater than the shortest distance in the crease pattern. Thus, this folding cannot exist.

The only way to increase the length of the red line (shortest distance) without increasing the length of the blue line (intrinsic distance) is to add collapsed regions, which are shown in Figure 11 in gray. Anytime a collapsed region is added, a seam is created.  $\square$

Another property of a rectilinear polygon extrusion is its scale factor, as derived in Equation 7. Since the height-to-thickness ratio of a folded rectilinear polygon

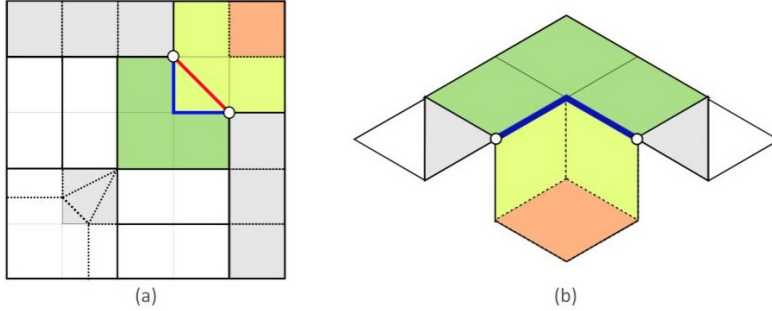


**Fig. 16** Visual representation of Theorem 1. (a) shows a hypothetical crease pattern for creating a 90° intersection gadget without seams, and (b) shows a hypothetical folded version of (a).

extrusion is given, the only variables constraining the scale factor of the rectilinear polygon extrusion are the widths of the collapsed regions.<sup>6</sup> However, as we prove below, the width itself of the collapsed regions is constrained by another factor, the height-to-thickness ratio, and our crease patterns indeed have the highest efficiency, i.e., they produce the smallest possible scale factor.

**Theorem 2** *No set of watertight, orthogonal gadgets with a thickness greater than zero and at least one 90° vertex can have a scale factor smaller than  $s$  as defined in Equation 7.*

*Proof* The scale factor of a folded rectilinear polygon extrusion with a specified height-to-thickness ratio is determined by the width of the collapsed region,  $w$ . In our crease patterns, the width  $w$  is equal to  $\frac{d}{2} = \frac{h}{r}$ , where  $d$  is the intrinsic distance,  $h$  is the height of the model, and  $r$  is the height-to-thickness ratio. Consider the crease pattern shown in Figure 17 (a), where  $w$  is less than  $\frac{d}{2}$ . The shortest possible length

---

<sup>6</sup>It may be tempting to calculate the minimum width  $w$  of a collapsed region, where  $d$  is the intrinsic distance, by setting the intrinsic distance equal to the shortest distance as follows:

$$\begin{aligned}
 d &= \left(\frac{d}{2} + w\right) \cdot \sqrt{2} \\
 d \cdot \frac{\sqrt{2}}{2} &= \frac{d}{2} + w \\
 w &= \frac{d}{2} \cdot (\sqrt{2} - 1)
 \end{aligned} \tag{8}$$

which is less than the width of the collapsed regions shown in Figure 11, equal to  $\frac{d}{2}$ . Thus, it may seem that our crease patterns are not the most efficient.

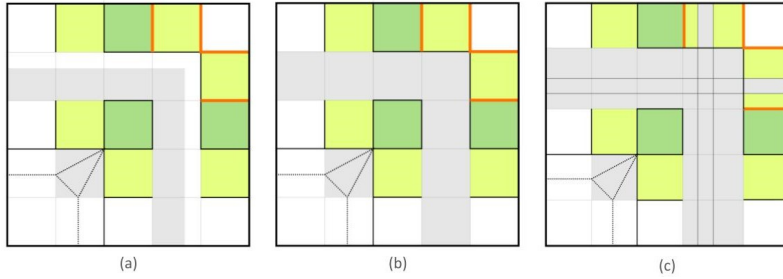


**Fig. 17 Visual representation of Theorem 2.** (a) shows a crease pattern with a collapsed region of  $w < \frac{h}{r}$ , (b) shows a crease pattern with a collapsed region of  $w = \frac{h}{r}$ , and (c) shows a crease pattern with a collapsed region of  $w > \frac{h}{r}$ . Green, yellow, white, and gray regions indicate faces, walls, non-extruded regions, and collapsed regions, respectively. All the crease patterns shown have an height-to-thickness ratio  $r$  of 1.

of paper between the lines marked in orange is a segment without any collapsed regions, with a length equal to the height  $h$  of the model. If the width  $w$  of the collapsed region is constrained so that  $w < \frac{d}{2} = \frac{h}{r}$ , like the expression derived in Equation 8, the edge of the collapsed region does not map to the boundary of the non-collapsed region. Thus, this crease pattern cannot be folded.

On the other hand, gadgets with an inefficient scale factor can be created, where  $w > \frac{d}{2} = \frac{h}{r}$ , as shown in Figure 17 (c). For the height of the gadget to remain as  $h$ , a collapsed region with width  $w - h$  can be added in the middle of the region between the orange lines.

Thus, the smallest possible width of the collapsed region is  $w = \frac{d}{2} = \frac{h}{r}$ , which is the width in our gadgets, as shown in Figure 17 (b). This demonstrates that the scale factor  $s$  of our models is the smallest possible scale factor of any folded rectilinear polygon extrusion.  $\square$

## 5 Conclusion

In this paper, we present a method for generating crease patterns corresponding to any origami rectilinear polygon extrusion with the specified thickness (i.e., uniform minimum edge-to-edge distance). We further derive the corresponding scale factor

$s$  of the folded rectilinear polygon extrusions generated under our method and prove that it is always less than  $1 + h$ , where  $h$  is the height of the model. Moreover, we prove that no rectilinear polygon extrusions with non-zero thickness can be seamless, and that rectilinear polygon extrusions generated under our method achieve the most efficient (smallest) scale factor possible. Finally, we develop a Python-based code implementation of our method.

Our method complements those of Demaine, Demaine, and Ku (2010) and Demaine, Ku, and Yoder (2018), which create graph-like models, by allowing for the customized creation of rectilinear polygon extrusions using a similar methodology. Specifically, whereas previous methods create graph-like models by layering gadgets at every edge intersection, our approach creates rectilinear polygon extrusions by layering newly-designed gadgets at every “square” within the 2D polygon. As a result, it facilitates the design of a broader range of geometric origami models, particularly those with repeating and symmetric patterns.

Furthermore, the various topological properties of the models generated using our gadgets make them ideal tactile tools for mathematical study. For example, a generalization of the theorems concerning a specific type of rectilinear polygon extrusions presented in our paper to all rectilinear polygon extrusions could serve as an engaging exercise for those interested in mathematics and origami.

Lastly, by enabling the efficient creation of complex designs from a flat, continuous sheet of material, the models generated by our method may have broad applications beyond mathematical origami and could potentially contribute to the design of foldable structures that are lightweight, compact, and manufacturable. For instance, the creases produced by our method could be replicated using laser-cut live hinges. Therefore, our method has important implications for not only the design, pedagogy, and mathematical exploration of origami, but also related fields such as aerospace, biomedical, and mechanical engineering.

## Appendix A: Sample Folded Models

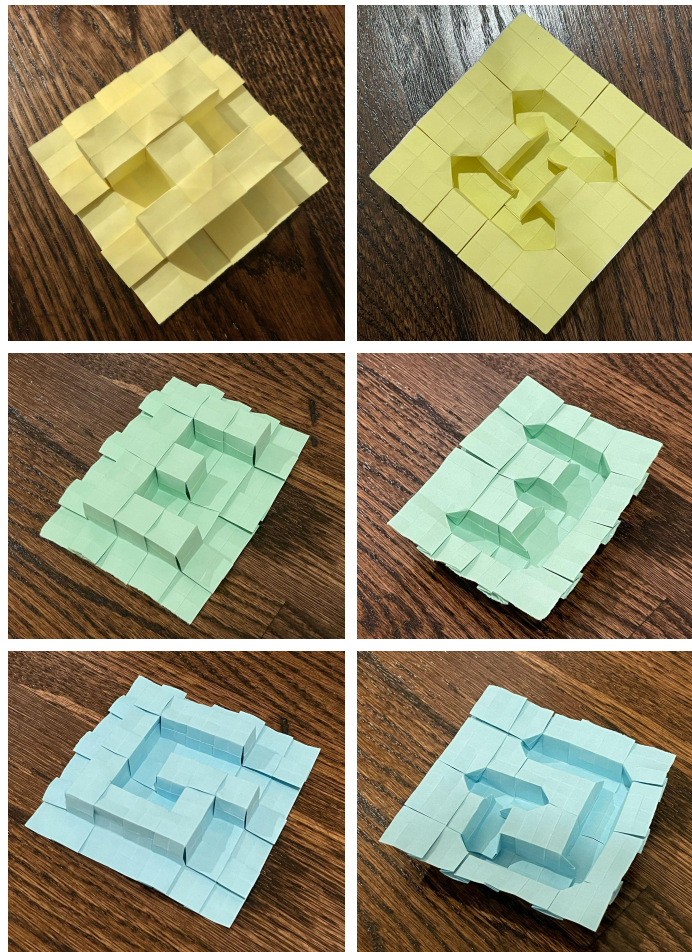


**Fig. A1** Rectilinear polygon extrusions of the letters “H,” “E,” and “G,” with a height-to-thickness ratio of 1:1, generated by our method.

## Appendix B: Code Implementation

In this section, we introduce a Python-based code that implements the method described in the paper.<sup>7</sup> Figure 4 shows the overall process of our method, which is open access through [GitHub](#).

Under our code implementation, one needs to first enclose a 2D rectilinear polygon within a padding with width equal to that of one square (Figure B1 a). This ensures that all ends of the folded rectilinear polygon extrusion are closed in the generated crease pattern. Our code runs in linear time relative to the number of squares in the padded model (for example, 24 squares in Figure B1 a).

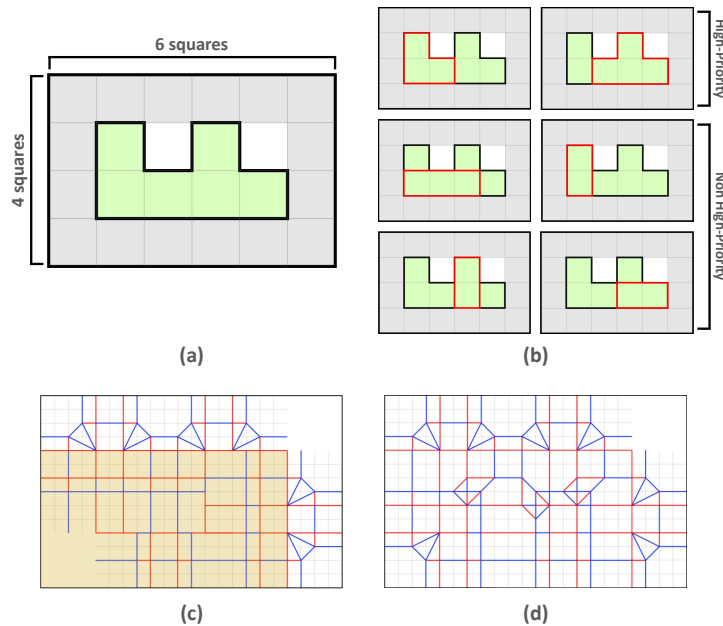


**Fig. B1 Example of a given 2D rectilinear polygon and its division into gadgets.** (a) illustrates a 2D rectilinear polygon, filled in light green, and a padding of width one square, filled in gray. (b) illustrates the division of the model into gadgets. (c) shows the crease pattern with only non high-priority gadgets layered (bottom two rows of panel b). Orange areas indicate areas about to be “overwritten” by crease patterns from high-priority gadgets.

---

<sup>7</sup>Other than a few modified steps in layering and connecting gadgets to allow the program to run more efficiently, the code implementation produces the same result as the method described in the main text.

By selecting a gadget for every square in the 2D rectilinear polygon, we obtain as many gadgets as squares in the 2D rectilinear polygon (Figure B1 b). With the exception of the  $n = 0$  gadgets, all gadgets presented in Figure 10 are used in rectilinear polygon extrusions. Many of these gadgets will overlap completely; for example, the 2D rectilinear polygon composed of six squares shown in Figure B1 (a) can be represented by only two gadgets (top row of Figure B1 b). While the human eye may intuitively recognize that the remaining four gadgets (middle and bottom rows of Figure B1 b) are completely overlapped, a code analysis of overlapping gadgets would not run in linear time relative to the number of squares in the padded model.

To optimize the efficiency of our code such that it runs in linear time, we implement a prioritization scheme for gadgets. Gadgets with extruded, non-central squares placed at  $90^\circ$  relative to the central square contain special sets of folds in their collapsed regions to allow for the  $90^\circ$  “bend.”<sup>8</sup> Thus, they are deemed *high-priority* gadgets. Other gadgets are placed on the crease pattern before high-priority gadgets. In areas where their crease patterns overlap, the creases of high-priority gadgets override those of other gadgets (Figures B1 c-d).

An added benefit of this method is that there is no need for any additional capping procedure. The code recognizes each end as an  $n = 1$  gadget. Since an  $n = 1$  gadget contains a single capped end and is not a high-priority gadget, when high-priority gadgets overlap with this  $n = 1$  gadget, their ends appear capped in the crease pattern (Figures B1 c-d).

We also implement sub-priorities for gadgets that are not deemed high-priority ones (i.e., non-high-priority gadgets). In certain circumstances, if two adjacent non-high-priority gadgets overlap incorrectly, a crease misalignment may occur (Figures B2 a and c). Thus, if one such gadget is directly adjacent to an  $n = 1$ ,  $n = 2$ , or  $n = 3$  gadget, it takes sub-priority over its non-high-priority neighbors, ensuring a correct crease alignment (Figures B2 b and d). Figure B2 (e) shows the complete order of priority for all gadgets.

---

<sup>8</sup>The top-left, bottom-middle, and bottom-right of Figure 11 show such gadgets.

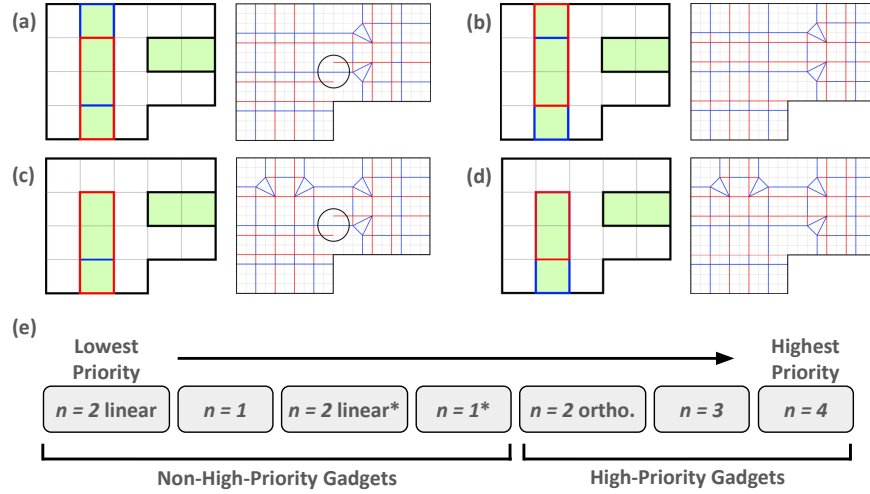


**Fig. B2** Prioritization scheme for non-high-priority gadgets. (a) and (b) illustrate a snapshot of a larger rectilinear polygon extrusion involving two overlapping  $n = 2$  gadgets, where the gadget highlighted in red takes priority over the one highlighted in blue. (a) demonstrates an incorrect prioritization between the two highlighted gadgets, resulting in a crease misalignment (black circle). (b) demonstrates a correct prioritization. (c) and (d) illustrate a similar snapshot involving priority between an  $n = 1$  and an  $n = 2$  gadget, where the gadget highlighted in red takes priority over the gadget highlighted in blue. (c) demonstrates an incorrect prioritization between the two highlighted gadgets, resulting in a crease misalignment (black circle). (d) demonstrates a correct prioritization. (e) shows the complete gadget order of priority with an asterisk denotes sub-priority.

After the gadgets are placed in the correct order, remaining paper not covered by any gadgets contains filler creases.<sup>9</sup> The final crease pattern is exported as a .svg file.

## References

- [1] Robert Lang, “Origami and Geometric Constructions,” in *Tokyo: Gallery Origami House*, vol. 68, 2010.
- [2] Erik D. Demaine, Martin L. Demaine, and Jason Ku, “Folding any orthogonal maze,” in *Origami<sup>5</sup>: Proceedings of the Fifth International Conference on Origami*

---

<sup>9</sup>These are creases that do not form any extrusions, but rather, collapse the paper to match the scale factor of the gadgets.

*in Science, Mathematics, and Education (OSME 2010)*, A K Peters, Singapore, 2010, pages 449-454.

- [3] Erik D. Demaine, Jason S. Ku, and Madonna Yoder, “Folding triangular and hexagonal mazes,” in *Origami<sup>7</sup>: Proceedings of the Seventh International Conference on Origami in Science, Mathematics, and Education (OSME 2018)*, vol. 2, Tarquin, Oxford, England, 2018, pages 647-652.
- [4] Erik D. Demaine and Tomohiro Tachi, “Origamizer: A practical algorithm for folding any polyhedron,” in *Proceedings of the 33rd International Symposium on Computational Geometry (SoCG 2017)*, vol. 77, Brisbane, Australia, 2017, pages 34:1-34:15.
- [5] Shannon A. Zirbel, Brian P. Trease, Mark W. Thomson, Robert J. Lang, Spencer P. Magleby, and Larry H. Howell, “HanaFlex: A large solar array for space applications,” in *Micro- and Nanotechnology Sensors, Systems, and Applications VII*, Proceedings of the International Society for Optics and Photonics, vol. 9467, International Society for Optics and Photonics, Maryland, 2015, page 94671; doi:10.1117/12.2177730.